RESEARCH ARTICLE

Molecular cloning and characterization of pirarucu (*Arapaima gigas*) follicle-stimulating hormone and luteinizing hormone β-subunit cDNAs

Thais Sevilhano[1], Roberto Feitosa de Carvalho[1], Nélio Alessandro de Jesus Oliveira[1], João Ezequiel Oliveira[1], Vinicius Gonçalves Maltarollo[2], Gustavo Trossini[2], Riviane Garcez[3], Paolo Bartolini[1]*

1 Biotechnology Department, IPEN-CNEN/SP, Cidade Universitária, São Paulo, SP, Brazil, 2 Department of Pharmacy, Faculty of Pharmaceutical Sciences, University of São Paulo, São Paulo, Brazil, 3 Genetic Ichthyology Laboratory, Bioscience Institute, University of São Paulo, São Paulo, SP, Brazil

* pbartoli@ipen.br

Abstract

The common gonadotrophic hormone α-subunit (GTHα) has been previously isolated by our research group from *A. gigas* pituitaries; in the present work the cDNA sequences encoding FSHβ and LHβ subunits have also been isolated from the same species of fish. The FSH β-subunit consists of 126 amino acids with a putative 18 amino acid signal peptide and a 108 amino acid mature peptide, while the LH β-subunit consists of 141 amino acids with a putative 24 amino acid amino acid signal peptide and a 117 amino acid mature peptide. The highest identity, based on the amino acid sequences, was found with the order of Anguilliformes (61%) for FSHβ and of Cypriniformes (76%) for LHβ, followed by Siluriformes, 53% for FSHβ and 75% for LHβ. Interestingly, the identity with the corresponding human amino acid sequences was still remarkable: 45.1% for FSHβ and 51.4% for LHβ. Three dimensional models of ag-FSH and ag-LH, generated by using the crystal structures of h-FSH and h-LH as the respective templates and carried out via comparative modeling and molecular dynamics simulations, suggested the presence of the so-called "seat-belt", favored by a disulfide bond formed between the 3rd and 12th cysteine in both β-subunits. The sequences found will be used for the biotechnological synthesis of *A. gigas* gonadotrophic hormones (ag-FSH and ag-LH). In a first approach, to ascertain that the cloned transcripts allow the expression of the heterodimeric hormones, ag-FSH has been synthesized in human embryonic kidney 293 (HEK293) cells, preliminarily purified and characterized.

Introduction

The two pituitary gonadotrophic hormones, follicle-stimulating hormone (FSH) and luteinizing hormone (LH), are strictly related to gonadal development and differentiation, regulating reproductive processes such as gametogenesis and follicular growth in all vertebrates, fish

included [1–4]. These hormones can thus be employed as spawning inductors to improve breeding and set up reproductive centers, which is particularly important for endangered and overexploited species of fish used for human consumption, like *Arapaima gigas* [5–8].

Gonadotrophic hormones (GTHs) are non-covalently bound heterodimeric glycoproteins composed of a common α-subunit, important for signal transduction, protein folding and heterodimer stabilization, and a hormone-specific β-subunit that influences secretion, disulfide bond pairing, metabolic clearance rate and elicits a particular biological response [9–12]. The folding, secretion, circulatory half-life, maintenance of heterodimer stability and biological potency of these glycoprotein hormones are also influenced by their carbohydrate moiety [13]. The N-linked oligosaccharides of most gonadotrophic hormones from a variety of species differ in branching and, especially, in two terminal modifications: sialylation and sulfation. These greatly influence the half-life of glycohormones, since sialylation protects them against clearance, while sulfation leads to a more rapid clearance rate upon binding to a receptor on the surface of liver endothelial cells [14]. The carbohydrate moiety, besides altering the pharmacokinetics of a given hormone, has also been shown to affect its receptor interactions. Human α-subunit Asn^{52} oligosaccharide, close to the putative receptor-binding region, seems in fact to exert a hormone-specific functional role in the hormone-receptor interaction and receptor activation [15].

As mentioned, the specificity of the hormone action is mostly determined by the β-subunit, but it is also known that determinants in the heterodimer account for the synthesis of hormone-specific carbohydrate structures. The diversity of the oligosaccharide structures finally synthesized indicates that the assembly of the α-subunit with the hormone-specific β-subunit, occurring in the endoplasmic reticulum, elicits a hormone-specific processing of N-linked oligosaccharides [14].

Following the pioneering work of Suzuki et al. [16] reporting the successful purification and characterization of two chemically distinct gonadotropins from chum salmon and the consequent proposal that there also existed two gonadotropins in teleosts, a large number of fish species have had their gonadotrophic hormones cloned and characterized. The cloning of the cDNAs of FSH and the LH α- and β-subunits of these species includes the Atlantic halibut [17], goldfish [18, 19], Russian sturgeon [20], rockfish [21], Manchurian trout [22], zebrafish [23], Senegalese sole [24], marbled eel [25], Chinese sturgeon [26], Atlantic cod [27] and sablefish [28]. Among these, Choi et al. [22], Huang et al. [25], Kim et al.[21] and So et al. [23] also presented phylogenetic trees including the α- and β-subunit of both gonadotropins. With regard to fish FSH and/or LH heterologous expression, of particular interest are the syntheses obtained via baculovirus in silkworm larvae for goldfish [29] and those in the yeast *Pichia pastoris* for Japanese eel [30], tilapia [31,32] and zebrafish [33]. Either stable or transient CHO expression of both gonadotropins was also obtained for Manchurian trout [22] and for zebrafish [23]. With the exception of Kazeto's group, who synthesized and purified Japanese eel [34] and channel catfish [35] FSH and LH obtained in the S2 drosophila cell line, the synthesized recombinant gonadotropins were not extensively purified and characterized in most of these works, being mainly analyzed via SDS-PAGE and Western blotting and tested in different bioassays. None of the above-mentioned species of fish, moreover, are representative of the order of Osteoglossiformes and not even of the superorder of Osteoglossomorpha, to which *A. gigas* belongs.

Arapaima gigas (pirarucu) is a giant Arapaimidae native to the Amazon River basin that can reach 3 meters in length and weigh up to 250 kg, present in Brazil, Ecuador, Colombia, Peru and Bolivia. This species is in danger of disappearing because of the exploitation by the fishing industry and increasing human presence [5]. It is largely used for food and extractivism purposes and commercial breeding is still incipient. In previous work, our research group isolated and characterized the cDNA of the α-subunit of *A. gigas* gonadotropins encoding for a

115 amino acid glycoprotein with a signal peptide of 24 and a mature peptide of 91 amino acids and also carried out a phylogenetic analysis based on its amino acid sequence [36]. In the present work, the cDNAs of ag-FSHβ and of the ag-LHβ have also been isolated from *A. gigas* pituitaries and sequenced for future biotechnological synthesis of these gonadotrophic hormones, useful for physiology and fertility studies and related applications. A three dimensional comparative modeling and a phylogenetic analysis, based on the two different β-subunit transcripts, was also carried out. As a first approach, ag-FSH has also been synthesized in HEK293 cells and preliminarily characterized.

Materials and methods

The project was approved by the Animal Ethic Commission of our Institution. Licenses were obtained from the Brazilian Institute of Environment (IBAMA), Reg. N˚ 5198393; Regional Council of Veterinary Sciences, Reg. N˚ 32242-PJ and Ministry of Fishery and Aquiculture, Reg. N˚ 00755-SP. Pituitaries were processed and stored in the Tissue Bank of the Genetic Ichtiology Laboratory of the University of Sao Paulo.

Animals

Six pirarucus (*A. gigas*), two males and four females, 2–4 years old, with total length between 100 and 140 cm and weighing 15–40 kg, were obtained in a commercial fishing station in the district of São João da Boa Vista, SP, Brazil (21˚ 58' 09" latitude South and 46˚ 47' 53" longitude West), to which the remains of the fish carcasses were returned. Pirarucus were caught from small lakes by the station personnel, using appropriate fishing nets. After decapitation, carried out by the same personnel under the supervision of our group and, in particular, of one of the authors belonging to the Genetic Ichtiology Laboratory of the Biological Science Institute of the University of São Paulo, pituitary glands were immediately removed following decapitation, stored in "RNA later solution" (Life Technologies), and transported to São Paulo for the experiments. Pituitaries were processed and stored in the Tissue Bank of the Genetic Ichthyology Laboratory of the University of São Paulo. The FSHβ and LHβ subunit transcripts were repeatedly analyzed, using at least 3 different pituitaries per each region of the gene.

Total RNA extraction

Total RNA was extracted from individual pituitary glands (wet weight: 70–100 mg) of *A. gigas* using the Purelink® total RNA Mini purification kit (Life Technologies, Carlsbad, CA, USA) and kept at the temperature of -70˚C.

Reverse-transcribed polymerase chain reaction (RT-PCR) and design of consensus or degenerated primers

All oligonucleotides used as primers were designed employing the Bio Edit® software [37]. Initially, nine (FSHβ) and six (LHβ) primer pairs were designed based on the conserved regions of 26 (FSHβ) and 25 (LHβ) fish sequences deposited in the GenBank, chosen among the species listed in Table 1, and these were used for different PCR test reactions. Complementary DNA (cDNA) was obtained from 0.25 μg of total pituitary RNA extracted from individual pituitary glands, using a GoScript® Reverse Transcription System (Promega, Madison, WIS, USA). After Oligo-dT and Random Primer addition, incubation was performed at 70˚C for 5 min. GoScript® Reverse Transcriptase was then added before annealing at 25˚C for 5 min, extending the reaction for 1 h at 42˚C. Inactivation was carried out at 70˚C for 15 min. PCR was performed in a Veriti 96-well Thermocycler (Applied Biosystems®, Foster City, CA,

Table 1. Fish species and Genbank accession numbers for the sequences used in the amino acid percentage identity and phylogenetic analyses of the FSH and LH glycoprotein beta subunits.

Organism	LH		FSH		
	Nucleotide (mRNA)	Amino acid	Nucleotide (mRNA)	Amino acid	
Arapaima gigas	KJ741848	this paper	KJ729119	this paper	Osteoglossomorpha, Osteoglossiformes, Arapaimidae
Acipenser baerii	AJ251656	CAB93502	AJ251658	CAB93504	Chondrostei, Acipenseriformes, Acipenseridae
Acipenser schrenckii	AY575921	AAS92239	AY575920	AAS92238	Chondrostei, Acipenseriformes, Acipenseridae
Acipenser sinensis	EU523733	ACB29495	EU523732	ACB29494	Chondrostei, Acipenseriformes, Acipenseridae
Anguilla anguilla	X61039	CAA43374	AY148427	AAN64352	Elopomorpha, Anguilliformes, Anguillidae
Anguilla japonica	AB175835	BAD14302	AB016169	BAA36546	Elopomorpha, Anguilliformes, Anguillidae
Anguilla marmorata	FJ490347	ACK87153	FJ490346	ACK87152	Elopomorpha, Anguilliformes, Anguillidae
Conger myriaster	AB045158	BAB97391	AB045157	BAB97390	Elopomorpha, Anguilliformes, Congridae
Misgurnus anguillicaudatus	AB603807	BAK39639	AB603806	BAK39638	Ostariophysi, Cypriniformes, Cobitidae
Carassius auratus	D88024	BAA13531	D88023	BAA13530	Ostariophysi, Cypriniformes, Cyprinidae
Ctenopharyngodon idella	EF565171	ABQ51327	EF552359	ABQ42694	Ostariophysi, Cypriniformes, Cyprinidae
Danio rerio	AY424304	AAR84283	AY424303	AAR84282	Ostariophysi, Cypriniformes, Cyprinidae
Hypophthalmichthys nobilis	EF565164	ABQ42715	EF552360	ABQ42695	Ostariophysi, Cypriniformes, Cyprinidae
Pimephales promelas	DQ242617	ABB51645	DQ242616	ABB51644	Ostariophysi, Cypriniformes, Cyprinidae
Clarias gariepinus	X97761	CAA66359	AF324541	AAN75753	Ostariophysi, Siluriformes, Clariidae
Ictalurus punctatus	AF112192	AAG32156	AF112191	AAG32155	Ostariophysi, Siluriformes, Ictaluridae
Silurus meridionalis	AY973946	AAY42269	AY973947	AAY42270	Ostariophysi, Siluriformes, Siluridae
Coregonus autumnalis	L23431	AAA68207	L23432	AAA68208	Protacanthopterygii, Salmoniformes, Salmonidae,
Brachymystax lenok	AY515501	AAR99811	AY515500	AAR99810	Protacanthopterygii, Salmoniformes, Salmonidae
Oncorhynchus mykiss	AB050836	BAB17687	AB050835	BAB17686	Protacanthopterygii, Salmoniformes, Salmonidae
Gadus morhua	DQ402374	ABD62884	DQ402373	ABD62883	Paracanthopterygii, Gadiformes, Gadidae
Odontesthes bonariensis	AY319833	AAP85607	AY319832	AAP85606	Acanthopterygii, Atheriniformes, Atherinopsidae
Fundulus heteroclitus	M87015	AAB59963	M87014	AAB59962	Acanthopterygii, Cyprinodontiformes, Fundulidae
Trichogaster trichopterus	AF157631	AAD51935	AF157630	AAD51934	Acanthopterygii, Perciformes, Osphronemidae
Trachurus japonicus	KC787605	AGO59025	KC787604	AGO59024	Acanthopterygii, Perciformes, Carangidae
Channa maculata	AY447037	AAS01609	AY447038	AAS01610	Acanthopterygii, Perciformes, Channidae
Haplochromis burtoni	HQ147565	ADQ42414	HQ147566	ADQ42415	Acanthopterygii, Perciformes, Cichlidae
Oreochromis niloticus	AY294016	AAP49576	AY294015	AAP49575	Acanthopterygii, Perciformes, Cichlidae
Pseudolabrus sieboldi	AB300391	BAF81901	AB300390	BAF81900	Acanthopterygii, Perciformes, Labridae
Amphiprion melanopus	FJ868868	ACR08088	FJ868867	ACR08087	Acanthopterygii, Perciformes, Pomacentridae
Dicentrarchus labrax	AF543315	AAN40507	AF543314	AAN40506	Acanthopterygii, Perciformes, Moronidae
Morone saxatilis	L35096	AAC38019	L35070	AAC38035	Acanthopterygii, Perciformes, Moronidae
Epinephelus coioides	AF507939	AAM28896	AY553982	AAS60199	Acanthopterygii, Perciformes, Serranidae
Acanthopagrus schlegelii	EF605276	ABQ96864	AY921613	AAX18926	Acanthopterygii, Perciformes, Sparidae
Pagrus major	AB028213	BAB18564	AB028212	BAB18563	Acanthopterygii, Perciformes, Sparidae
Scomber japonicus	JF495133	AEN14605	JF495132	AEN14604	Acanthopterygii, Perciformes, Scombridae
Thunnus thynnus	EF205591	ABP04050	EF208026	ABP04057	Acanthopterygii, Perciformes, Scombridae
Paralichthys olivaceus	AB042423	BAB47388	AB042422	BAB47387	Acanthopterygii, Pleuronectiformes, Paralichthyidae
Solea senegalensis	EU100410	ABW81404	EF617342	ABU95601	Acanthopterygii, Pleuronectiformes, Soleidae
Sebastes schlegelii	AY609080	AAU14142	AY609079	AAU14141	Acanthopterygii, Scorpaeniformes, Sebastidae
Monopterus albus	EU840258	ACF70665	JN381164	AET99103	Acanthopterygii, Synbranchiformes, Synbranchidae

USA) with 0.2 μM (final concentration) of sense and antisense primers and 5.0 U of Taq DNA polymerase hf (Life Technologies). After an initial 2 min denaturation step at 94°C, thirty-five cycles were carried out: denaturation at 94°C for 30 s, annealing at 54°C (FSHβ) or 57°C (LHβ) for 30 s and extension at 68°C for 1 min. Final elongation was at 68°C for 5 min before holding at 4°C. In the case of FSHβ, one pair of consensus primers (#1 and #2, Table 2) provided 3 PCR fragments on 1.2% agarose gel, the least intense being confirmed to correspond to a putative partial FSHβ sequence, located approximately in the central region of the cDNA. In the case of LHβ, one pair of degenerate primers (#10 and #11) provided a single PCR fragment that corresponded to a putative partial LHβ sequence. Partial sequences of ag-FSHβ- and ag-LHβ-subunit cDNA were thus ready to use for the following reaction.

Rapid amplification of cDNA ends (RACE) for FSHβ and LHβ sequencing

For 5'-RACE and 3'-RACE, 0.5 μg of total RNA were reverse-transcribed with 200 U of Superscript II (Life Technologies), either for FSHβ or LHβ sequencing.

In the case of FSHβ, gene-specific primer #3 was used for 5'-RACE, according to kit instructions, to get a single-stranded cDNA. The Abridged Anchor Primer (#5) was then used together with gene-specific primer #4 to obtain a PCR fragment that was finally purified and re-amplified using specific primer #4 and the Abridged Universal Amplification Primer (#6) from the kit. This finally provided a 356 bp sequence corresponding to the 5' region of FSHβ cDNA. The Adapted Primer (#7) was used for 3'RACE for obtaining single-stranded cDNA, according to kit instructions. The gene-specific primer #8 was then used together with the Abridged Universal Amplification Primer (#6). A single intense PCR fragment was obtained, which provided a 370 bp correct sequence corresponding to the 3' region of FSHβ cDNA. To confirm the whole FSHβ cDNA sequence, gene-specific primer #9, designed right at the beginning of the 5'-UTR sequence was used together with the Abridged Universal Amplification Primer.

In the case of LHβ, the 3'-RACE strategy was applied first, since, via degenerate primers, a sequence apparently closer to the 3' region had been obtained in the first phase. Adapted

Table 2. Primers used in cloning *A. gigas* FSHβ and LHβ subunits cDNAs.

Number	Direction	Name	Sequence
Primer 1	Sense	FSHβ consensus-1	5' ATG CAG CTG GTT GTC ATG GCA 3'
Primer 2	Antisense	FSHβ consensus-2	5' TCT GGC CAC AGG GTA GGT GA 3'
Primer 3	Antisense	ag-FSHβ-1	5' ACA GGG TAG GTG AAA T 3'
Primer 4	Antisense	ag-FSHβ-2	5' GGG TCC ACT CCT TCA GGG 3'
Primer 5	Sense	AAP	5' GGC CAC GCG TCG ACT AGT ACG GGI IGG GII GGG IIG 3'
Primer 6	Sense or antisense	AUAP	5' GGC CAC GCG TCG ACT AGT AC 3'
Primer 7	Antisense	AP	5' GGC CAC GCG TCG ACT AGT ACT TTT TTT TTT TTT TTT T 3'
Primer 8	Sense	ag-FSHβ-3	5' CCC TGA AGG AGT GGA CCC 3'
Primer 9	Sense	ag-FSHβ-5'UTR	5' GCT GGT AGG AGT CCA ACA G 3'
Primer 10	Sense	LHβ degenerate-1	5' CTG GTG TTY CAR ACM WCC ATC T 3'
Primer 11	Antisense	LHβ degenerate-2	5' AGT CMG ASG TGT CCA TKG TG 3'
Primer 12	Sense	ag-LHβ-1	5' GGG CGT GAG GTA CGA GA 3'
Primer 13	Antisense	ag-LHβ-2	5' CAT TGA GGG AAC AAA ACT 3'
Primer 14	Antisense	ag-LHβ-3	5' TGA TAT TTA GGG TTC GGG TTA GTT C 3'
Primer 15	Sense	ag-LHβ-5'UTR	5' TAT CTC GGC TGC CGC TTG TT 3'

Primer (#7) was used for obtaining single-stranded cDNA. Gene-specific primer #12, together with the Abridged Universal Amplification Primer (#6), gave a single intense PCR fragment that, after sequencing, provided a 409 bp sequence corresponding to the 3' region of LHβ cDNA. Gene-specific primer #13 was then used for 5'-RACE, obtaining single stranded cDNA. Abridged Anchor Primer (#5), together with gene-specific primer #14, gave a single, intense PCR fragment that provided a 624 bp sequence corresponding to the 5' region of LHβ cDNA. To confirm the whole LHβ cDNA sequence, gene-specific primer #15, designed right at the beginning of the 5'-UTR sequence was used together with the Abridged Universal Amplification Primer (#6).

The complete amino acid sequences of ag-FSHβ and of ag-LHβ subunits were determined and putative signal peptides were predicted using the "Signal peptide 4.1 Software" [38].

Molecular modeling

The initial three dimensional (3D) models of ag-GTHα, ag-FSHβ and ag-LHβ were generated by employing the threading modeling method [39,40], carried out using the HHpred server [41] and Modeller Software [42–44]. Initially, the HHpred server generated 1D alignments for the GTHα, FSHβ and LHβ subunits with sequences of the three dimensional structures of the proteins available at the Protein DataBank (PDB), employing a global alignment method and matching the predicted secondary structure of the models. The sequence of ag-GTHα, from Faria et al. [36], and those of ag-FSHβ and ag-LHβ, obtained in the present work, were aligned with human FSH and human chorionic gonadotropin (hCG) available at the PDB under IDs 4ay9, chains a and b [45,46], and 1hcn, chain b [47], respectively. All templates showed 100% of probability and identity values >47% when compared to their respective models (S1 Table).

After the primary alignments of the 3 subunits, initial 3D models were constructed using the Modeller Software. The 5 lowest energy models were chosen from the 60 that were generated and employed to obtain the optimum model for Molecular Dynamics simulations by evaluating their stereochemical quality via Ramachandran plots [48]. Both heterodimers were constructed by superimposing each modeled subunit on its respective crystallographic template (4ay9 and 1hcn).

Molecular Dynamics simulation. After the construction of the initial FSH and LH dimer models, the Molecular Dynamics (MD) simulation of these two modeled hormones was performed. All the MD parameters were equal for the two models generated, the simulation being carried out by employing the GROMACS v.4.5.4 software [49, 50] and using an explicit solvation system in which water molecules were represented by a Simple Point Charge model. The protonation states of the charged groups were those at pH 7.0 and counterions were added to insure electrical neutrality of the system at 0.1M NaCl. The Gromos Force Field [51] was chosen for the MD simulations at constant temperature and pressure in a periodic truncated cubic box in which the minimum distance between any atom of the protein and the box wall was 2.0 nm. Initially, an energy minimization based on the steepest descent algorithm was performed; subsequently, 20 ps of MD simulation, fixing the backbone atom positions, were applied at a temperature of 310˚K to relax the system. Finally, an unrestrained MD simulation was performed for 20 ns at 310˚K to assess the stability of the structures. During all simulations, the temperature and pressure (1.0 bar) were maintained constant [52].

Structural analysis and validation. The final model, generated by the MD simulations, was checked using several GROMACS structural analyses, as well as Ramachandran plots generated with the Rampage server [48]. The pseudo-energy profile of the models was analyzed via the Verify 3D server [53] and ProSA-web [54]. It is also important to emphasize that all protocols performed were based on current literature [55–57].

Phylogenetic analysis

The phylogenetic analysis was carried out on the basis of MUSCLE alignments [58] of the mature peptide DNA sequences of the FSHβ and LHβ subunits of 41 fishes, including *A. gigas*. The species and sequences used are presented in Table 1 and were obtained from the GenBank/EMBL. The alignment and identity calculations between the pairwise sequences were carried out via Geneious 5.5.6 and the search for the best substitution model and the phylogenetic trees via MEGA 6 [59]. All positions containing gaps and missing data were not considered in the analysis. The DNA sequence alignments from FSHβ and LHβ were concatenated to generate trees based on the methods of Maximum Parsimony (MP) and Maximum Likelihood (ML), applying the HKY model [60] with Gamma parameter = 1.34. The bootstrap test [61] with 1,000 replicates was conducted for all analyses, and the three Chondrostei (*Acipenser* species) were set as outgroup. Branches with less than 50 percent of the bootstrap replicates were collapsed.

Synthesis of ag-FSH in human embryonic kidney 293 (HEK293) cells

The transient transfection and synthesis of ag-FSH was carried out using the Expi293^{TM} Expression System Kit (Life Technologies, Carlsbad, CA, USA), following the manufacturer's instructions. Briefly, each ag-FSH α- and β-subunit cDNA was separately inserted into a pcDNA^{TM} 3.4-TOPO$^{®}$ vector, adding then 30 μg of plasmid DNA (15 μg for each subunit vector) to ExpiFectamine^{TM} 293 Reagent, in Opti-MEM$^{®}$ I medium, incubating for 20–30 min at room temperature to obtain the DNA-ExpiFectamine^{TM} 293 Reagent complex. The mixture (3 ml) was finally added to a 125-ml Erlenmayer shaker flask containing 7.5 x 10^7 Expi293F^{TM} cells in Expi293^{TM} Expression Medium, to a final volume of 28.5 ml. A negative control flask was also prepared by adding 3 ml of Opti-MEM$^{®}$ I medium instead of the DNA-ExpiFectamine^{TM} Reagent complex. Transfection was thus carried out in a 37°C incubator with a humidified atmosphere of 8% CO_2 in air, in an orbital shaker rotating at 125 rpm. Approximately 16–18 hours post-transfection, Transfection Enhancer 1 and Transfection Enhancer 2 were added, thus reaching a final volume of 30 ml in each 125-ml flask. Media, containing the secreted recombinant protein of interest, were harvested beginning at approximately 48 hours post-transfection and assayed for recombinant protein expression.

Conditioned medium purification by reversed-phase HPLC (RP-HPLC)

The first purification step was carried out via RP-HPLC on a Vydac C4 column (300 Å pore size, 5 μm particle size, 25 cm x 4.6 mm I.D) from Grace-Vydac (Fisher Scientific, USA) by applying 5 ml of transfection conditioned medium. Elution and gradient conditions were those described in Loureiro et al. [62], that were specifically set up for running undissociated FSH heterodimer. Under the same conditions, 5 ml of the negative control of transfection were also chromatographed on the same RP-HPLC column.

Ag-FSH purification by high-performance size exclusion liquid chromatography (HPSEC)

The pool of ag-FSH-derived material, which was evidently not present in the negative control, was applied to a HPSEC G2000 SW column (60 cm x 7.5 mm I.D., particle size of 10 μm and pore size of 125 Å), purchased from Tosoh Bioscience (Tokyo, Japan), eluting as described [63]. A similar pool, obtained from the RP-HPLC negative control, was applied to the same HPSEC column. A reference preparation, human FSH-SIAFP-B-3 (lot # AFP7298A), from the National Hormone & Peptide Program (NHPP, Torrance, CA, USA), was also applied.

Fig 1. Nucleotide and deduced amino acid sequence of the cDNA encoding for the FSHβ-subunit of *A. gigas*. M, inside a square, start coding region; G, inside a rhombus, first amino acid of the mature peptide; N I T, inside a rectangle, glycosylation site; C, inside a circle, conserved cysteine residues; P, inside a triangle, conserved proline residues; attaaa, designated with a black square, polyadenylation signal; aaaaaaaaaaa, designated with a gray square, poly(A+) tail. GenBank Accession number: KJ729119.

https://doi.org/10.1371/journal.pone.0183545.g001

Ag-FSH dissociation into α- and β-subunits

For heterodimer dissociation of ag-FSH into its subunits we utilized a methodology previously set up for pituitary or recombinant human glycoprotein hormones (5–10 μg in 50–100 μl phosphate-buffered saline), incubating overnight at 37°C in 5M acetic acid [64].

Results

cDNA sequencing

The DNA sequences obtained via 3' and 5'-RACE using material from at least three different pituitary glands were compared and aligned. Overlapping enabled their proper joining into nucleotide sequences spanning the entire cDNA.

The *A. gigas FSHβ* cDNA sequence (Fig 1) was 913 bp in total length and had an open reading frame of 381 bp beginning with the first ATG codon at position 79 bp (78 bp 5'-UTR) and ending with the stop codon at position 457 bp, presenting a 434 bp 3'-UTR. A polyadenylation signal (ATTAAA) was recognized 13 bp upstream from the poly (A+) tail. The coding region translates into a polypeptide of 126 amino acids, while the cleavage site for the putative signal peptide was predicted to be between amino acids 18 and 19. This provides a mature peptide of 108 and a signal peptide of 18 amino acids. The proposed mature peptide of ag-FSHβ thus contains 12 conserved cysteines and 2 conserved prolines (Fig 1). A putative N-linked glycosylation site, the only one predicted, was identified at amino acid position (AA) 8–10 (NIT), while a second possible N-linked glycosylation site was lost at AA 25–27 (TTT), as can be seen in the alignment of the mature peptide of ag-FSHβ with the other 37 teleosts and 3 Acipenseriformes (Fig 2).

The *A. gigas* LHβ cDNA sequence (Fig 3) was 711 bp in total length and had an open reading frame of 426 bp beginning with the first ATG codon at position 47 bp (46 bp 5'-UTR) and with the stop codon at position 469, presenting a 221 bp 3'-UTR. A polyadenylation signal (AATAAA) was recognized 18 bp upstream from the poly (A+) tail. It is interesting to observe that the non-consensus polyadenylation signal ATTAAA, already found in ag-GTHα cDNA [36] and here confirmed in ag-FSHβ, was replaced in ag-LHβ cDNA by the very highly conserved AATAAA [65]. The coding region translates into a peptide of 141 amino acids, while
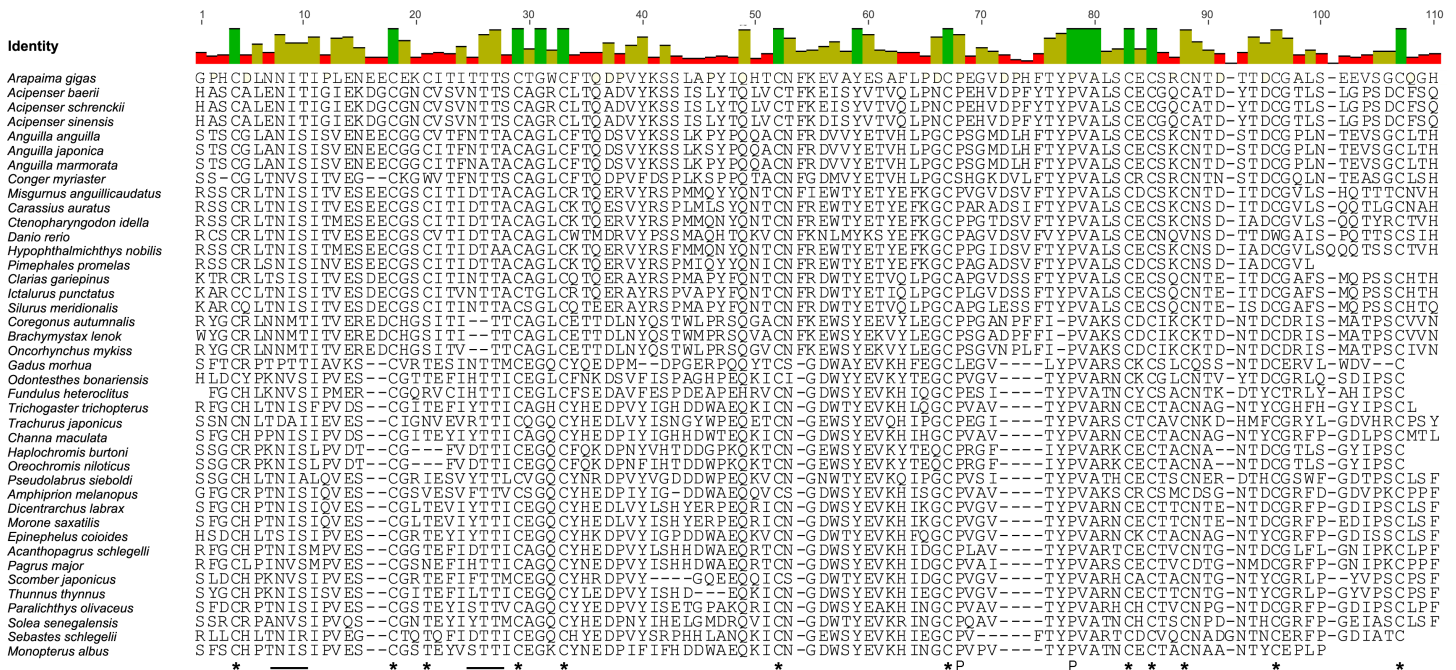
Fig 2. Alignment of the FSHβ mature peptides of three Chondrostei and 38 teleosts, including *A. gigas*. The Genbank accession numbers for these sequences are given in Table 1. Below the alignment the conserved cysteines(*), prolines (P) and the putative N-linked glycosylation sites (___) are highlighted.

the cleavage site for the putative signal peptide was predicted to be between amino acid 24 and 25. This provides a mature peptide of 117 and a signal peptide of 24 amino acids. The proposed mature peptide of ag-LHβ thus contains 12 conserved cysteines and 6 conserved prolines (Fig 3). A putative N-linked glycosylation site was identified at AA 10–12 (NQT), while a second possible N-linked glycosylation site was lost at AA 27–29 (QTT) of the mature peptide (Fig 4).

The comparison between the amino acid sequences of FSH and LH β-subunits of *A. gigas* reveals an identity of 49.5%. Table 3 presents the percent identities of LHβ and FSHβ mature peptides for 13 fish orders. The percent identities of the ag-FSHβ and ag-LHβ mature peptides, in comparison with the corresponding human sequences, were 45.1% and 51.4%, respectively.

Molecular modeling

Fig 5 displays in the upper part the average structure in solution of ag-FSH and ag-LH, highlighting the two subunits, the predicted disulfide bridges and the loops. The so-called "seat belt" in the β subunits, known to wrap around the α subunit, can also be identified between the 3rd and 12th cysteine: C39 and C123, for ag-FSH, and C47 and C131, for ag-LH. In the lower part of Fig 5, the 3D models are presented in cartoon style, highlighting the predicted secondary structures (helices and sheets) and the two residues located in the outlier regions of Ramachandran plots. In Fig 6 (top) the electrostatic potential surfaces of ag-FSH and ag-LH and the partial surfaces of the α- and β-subunits are shown. In Fig 6 (bottom) the proline residues, which were found to be conserved by comparing the four human and *A. gigas* gonadotropin sequences, are located in the β-sheet/loop regions.

Several structural parameters, such as the root-mean-squared deviation (RMSD) of the backbone atom positions indicating structural stability, the radius of gyration indicating protein compaction, the hydrophobic and hydrophilic surface areas indicating solvent exposure

Fig 3. Nucleotide and deduced amino acid sequence of the cDNA encoding for the LHβ-subunit of *A. gigas*. M, inside a square, start coding region; V, inside a rhombus, first amino acid of the mature peptide; N Q T, inside a rectangle, glycosylation site; C, inside a circle, cysteine residues; P, inside a triangle, proline residues; aataaa, designated with a black square, polyadenylation signal; aaaaaaaaaaa, designated with a gray square, poly(A+) tail. GenBank Accession number: KJ741848.

https://doi.org/10.1371/journal.pone.0183545.g003

and the number of hydrogen bonds between protein atoms (S1 Fig), confirmed that the structures of both hormones had stabilized by around 15 ns of MD simulation. The last 5 ns of simulation were thus analyzed. It is important to observe that, during the 20 ns simulation, physicochemical parameters such as the total energy, periodic box volume and pressure, temperature and density of the system were stable, showing only very small variations: this indicates the stability of the simulated system (S2 Table).
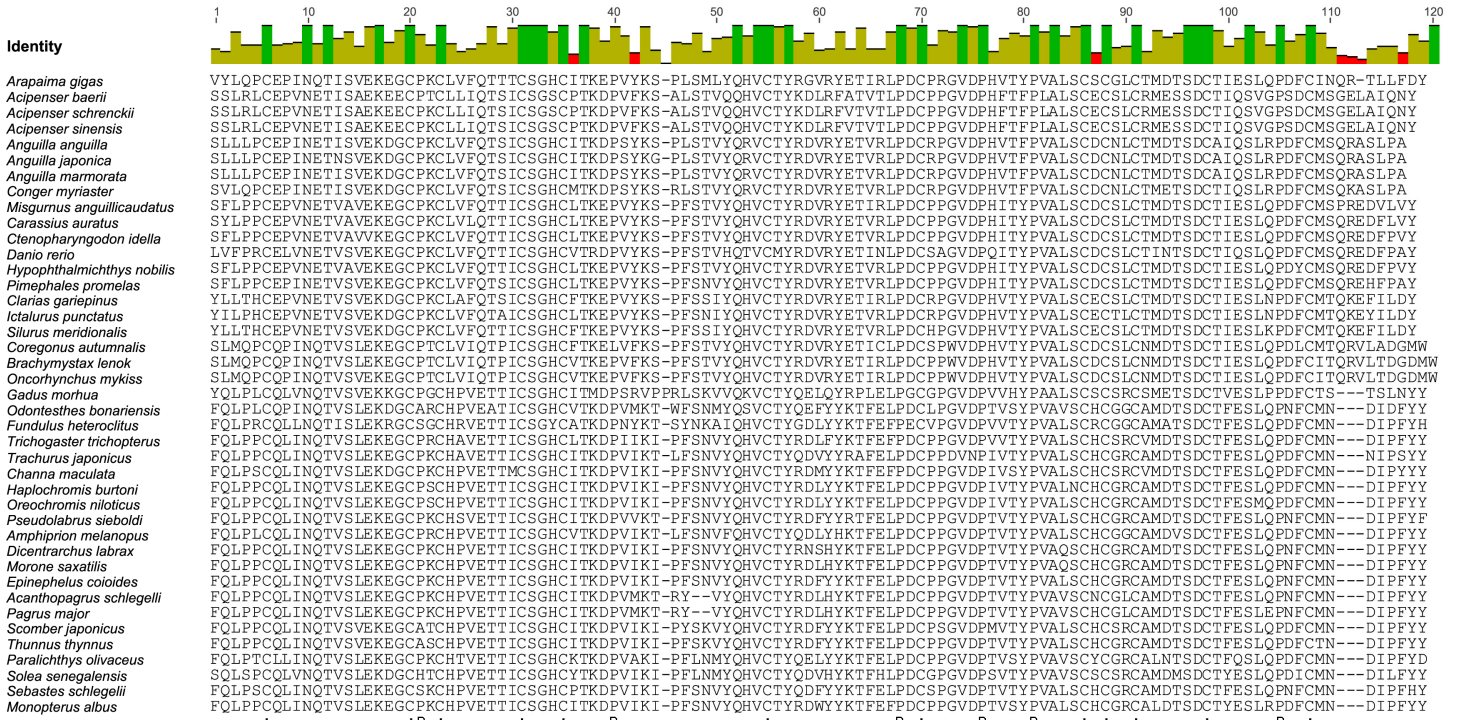

Fig 4. Alignment of the LHβ mature peptides of three Chondrostei and 38 teleosts, including *A. gigas*. The Genbank accession numbers for these sequences are given in Table 1. Below the alignment the conserved cysteines (*), prolines (P) and the putative N-linked glycosylation site (___) are highlighted.

https://doi.org/10.1371/journal.pone.0183545.g004

Table 3. Percentage identity of FSHβ and LHβ peptides among fish orders (FSHβ above the diagonal).

			1	2	3	4	5	6	7	8	9	10	11	12	13
1	Teleostei Osteoglossomorpha	Osteoglossiformes (*A. gigas*)	-	51.1	60.9	51.6	53.0	44.1	33.0	37.6	37.4	36.3	35.7	36.4	35.0
2	Chondrostei	Acipenseriformes (3)	55.6	-	48.7	44.7	49.4	39.0	27.8	35.2	33.9	33.4	32.0	32.4	33.3
3	Teleostei Elopomorpha	Anguilliformes (4)	74.3	64.7	-	54.4	56.6	43.8	33.2	41.0	40.6	39.0	39.8	36.1	39.7
4	Teleostei Ostaryophysi	Cypriniformes (6)	75.6	63.4	77.8	-	66.6	47.0	33.6	40.0	37.9	39.7	40.4	40.8	39.1
5	Teleostei Ostaryophysi	Siluriformes (3)	74.9	61.3	75.7	80.2	-	44.8	35.5	40.4	38.0	40.5	41.3	37.9	39.8
6	Teleostei Protacanthopterygii	Salmoniformes (3)	74.2	59.3	71.7	76.4	73.1	-	32.1	36.7	36.4	36.7	36.7	39.1	31.7
7	Teleostei Paracanthopterygii	Gadiformes (1)	53.8	48.7	52.1	53.3	54.9	49.7	-	49.0	41.0	48.5	49.1	45.2	49.0
8	Teleostei Acanthopterygii	Atheriniformes (1)	57.6	46.6	53.0	56.6	58.5	57.1	59.8	-	60.0	58.1	57.3	51.9	59.4
9	Teleostei Acanthopterygii	Cyprinodontiformes (1)	55.1	47.5	52.1	54.8	54.8	51.6	59.0	70.7	-	53.9	49.5	49.0	58.5
10	Teleostei Acanthopterygii	Perciformes (14)	65.1	52.4	59.7	65.5	63.0	63.5	63.5	80.5	74.7	-	63.0	56.0	66.4
11	Teleostei Acanthopterygii	Pleuronectiformes (2)	59.7	50.4	55.4	61.3	60.7	59.1	60.2	76.7	69.0	79.5	-	56.7	66.6
12	Teleostei Acanthopterygii	Scorpaeniformes (1)	62.7	51.4	57.9	63.3	61.9	61.9	61.5	83.6	75.0	88.9	80.6	-	59.2
13	Teleostei Acanthopterygii	Synbranchiformes (1)	64.4	50.5	60.2	64.7	62.7	62.2	62.4	79.3	73.3	89.5	81.0	88.8	-

https://doi.org/10.1371/journal.pone.0183545.t003

Both 3D models were validated with ProSA-web, all residues being found under 0 score, and with "Verify 3D", in which only the C-terminus of ag-LHβ was above 0 score; according to the Ramachandran plot, ag-LH presented only 2 residues that were outliers in the loop region (S3 Table).
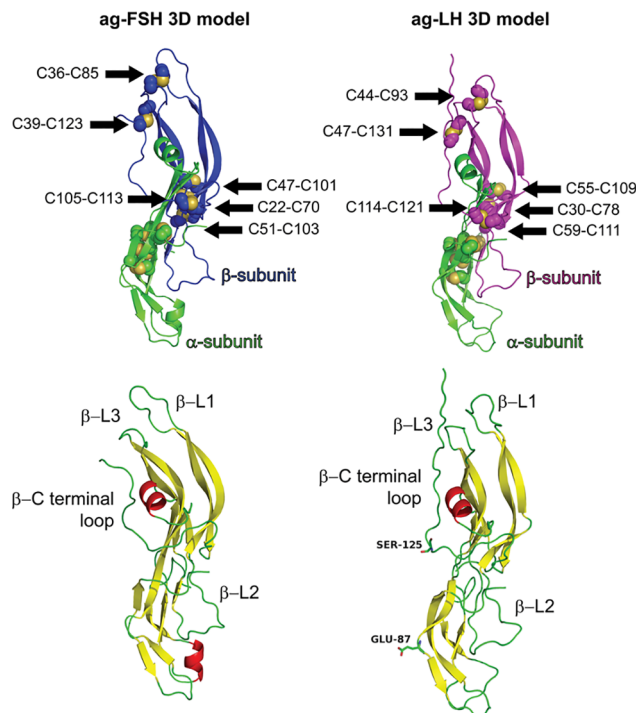
Fig 5. Tridimensional models obtained after molecular dynamics simulations. On the top, the ag-FSH and ag-LH structures highlighting the α-subunit (green cartoons) and the β-subunit (blue for FSH and magenta for LH) and the predicted dissulfide bonds of the β-subunits are shown. On the bottom, the 3D models are presented in cartoon style and colored according to the secondary structure (helices in red, sheets in yellow and loops in green), highlighting the predicted loops of the β-subunits and the residues predicted in the outlier regions of the Ramachandran plot.

https://doi.org/10.1371/journal.pone.0183545.g005

Fig 6. On the top, electrostatic potential surface of ag-FSH (left) and ag-LH (right) and surface of α- and β-subunits. The surface is colored in blue (positively charged groups) and red (negatively charged groups), while neutral groups are in white. The black arrow indicates the "seat-belt" structure of the β-subunits. On the bottom, localization of 5 (ag-FSH) and 7 (ag-LH) conserved pr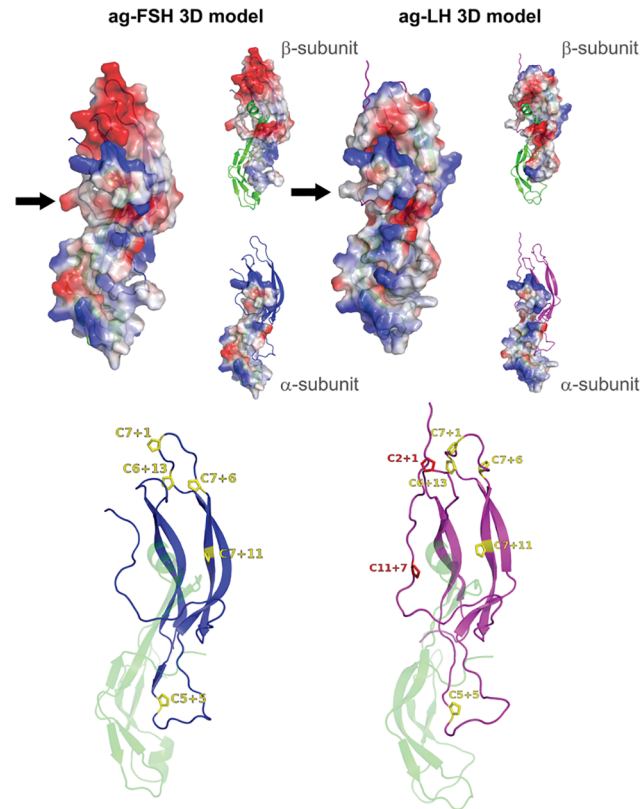oline residues in the hormone structures. Each proline is identified according to its position in relation to the previous cysteine residue.

https://doi.org/10.1371/journal.pone.0183545.g006

The calculated root-mean-square fluctuations (RMSF) of both hormones are shown in S2 Fig. As expected, the RMSF for the α subunits suggests that their backbones have almost identical profiles. In the case of the β subunits, minor differences in the RMSF values are observed, also suggesting similar backbone movements.

A comparison between the seat-belt amino acid composition of ag-LH, ag-FSH and all gonadotropins analyzed by Aizen et al. [66] is shown in S3 Fig.

Phylogenetic analysis

The combined analysis of FSHβ and LHβ DNA sequences presented in S4 Fig shows that most branches have high bootstrap support, except within the Acanthomorpha superorder, which is in fact collapsed in this figure. Although not shown in the figure, supports above 50% were found in Pleuronectiformes (above 80%) and in the Perciformes clades: Cichlidae (100%), Scombridae (above 95%), Moronidae (100%), Sparidae (100%), Moronidae+Sparidae (above 80%) and in the group formed by *Channa maculata* (Channidae) and *Trichogaster trichopterus* (Osphronemidae) (71.8% for ML and 60.2% for MP). Maximum parsimony also supports a clade formed by *Pseudolabrus sieboldi* (Labroidei, Labridae) and *Epinephelus coioides* (Percoidei, Serranidae) (76.3%) within Acanthomorpha. The overall phylogenetic relationships within the Acanthomorpha, however, could not be fully resolved.
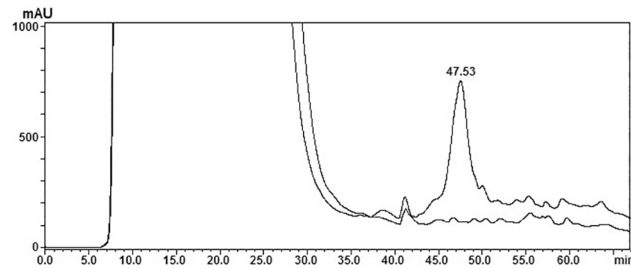
Fig 7. First purification step of HEK293F conditioned medium via RP-HPLC. The chromatogram is derived from the application of 5 ml of ag-FSH transfection conditioned medium, in comparison with an analogous chromatogram derived from the application of 5 ml of the negative control of transfection.

Ag-FSH synthesis in HEK293 cells

As shown in Fig 7, using a particular RP-HPLC condition that does not dissociate FSH hetero-dimer [62], ag-FSH-related material was obtained from HEK293 conditioned medium, while no material appeared in the same position when the negative control of transfection was run under the same conditions. A pool of this ag-FSH-related material was then purified twice on HPSEC, presenting a symmetrical peak whose t_R is quite close to that shown by the human FSH reference preparation, run under the same conditions (Fig 8). A complete dissociation of ag-FSH into its α- and β-subunit, after overnight incubation with 5M acetic acid, following an analogous protocol that we have previously described for hFSH subunit dissociation [64], provided a very similar pattern (Fig 9). A preliminary quantification concerning ag-FSH expression in this HEK293 cell line, adapted to high density, serum-free suspension culture, indicated a yield of ~28 mg/liter.

Discussion

The mature peptides of the two beta subunits (FSH and LH) are derived from the same ancestral gene [67,68] and the comparison between the amino acid sequences of the FSHβ and LHβ subunits of *A. gigas* reveals an identity of 49.5%, which is higher than that calculated for other fishes, ranging from 32 to 40% [19,23,69]. Besides the 12 conserved cysteines and the first N-glycosylation site (NxT), the other interesting conserved positions of FSHβ and LHβ in fishes are related to the second putative N-linked site (absent in both *A. gigas* beta subunits), to a conserved region between Cys7 and Cys8 and to the dimer interface positions, similar to what has been reported for other glycoprotein hormone beta chains [45,70]. In the position related to the second putative N-linked glycosite, both human forms, for example, present an active NTT site, while ag-FSHβ presents a TTT sequence and ag-LHβ a QTT sequence. As far as we know, the conserved region between the 7th and 8th Cys (relative to tetrapods) does not seem to be related to any known function. Interestingly, this region concentrates conserved proline residues that can be essential for the protein structure of gonadotropin beta subunits, since prolines tend to bend the regional amino acid alignment and therefore to fold the protein [71,72].

The main characteristic of the primary structure of the FSH and LH beta subunits is the presence of 12 conserved cysteines. These are important for determining the cysteine-knot structure comprising 3 disulfide bridges [14] for stabilizing the heterodimer [73] and for hormone activity [74–76]. The alignment of the mature peptides shows that this structure is highly conserved in fish LHβ subunits but not in FSHβ, which is less conserved both in structure and sequence [1]. The table of the percentage of amino acid identities clearly shows that FSHβ is more variable than LHβ (27.8–66.6% and 46.6–89.5%, respectively), which contrasts with
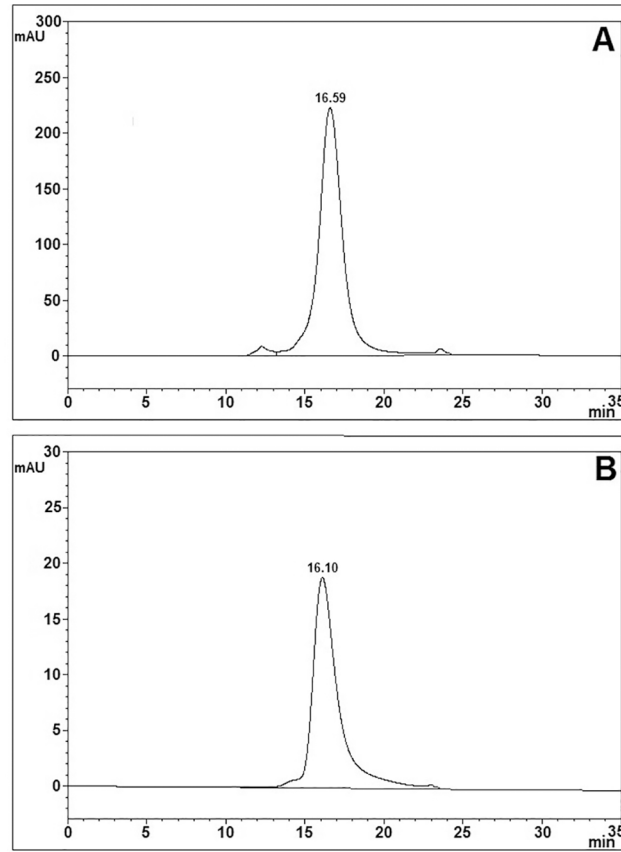
Fig 8. HPSEC obtained upon application of: (A) 0.25 ml of a pool of ag-FSH-derived material from RP-HPLC (see Fig 7) and already purified once on the same HPSEC; (B) 5μg/5μl of human pituitary FSH reference preparation from NHPP, run under identical conditions.

https://doi.org/10.1371/journal.pone.0183545.g008

Tetrapoda, where LHβ diverged faster than FSHβ. According to So et al. [23], the significantly lower conservation in fish FSHβ implies a functional divergence of FSH, and raises an interesting question about the roles and physiological relevance of FSH in different groups of teleosts.
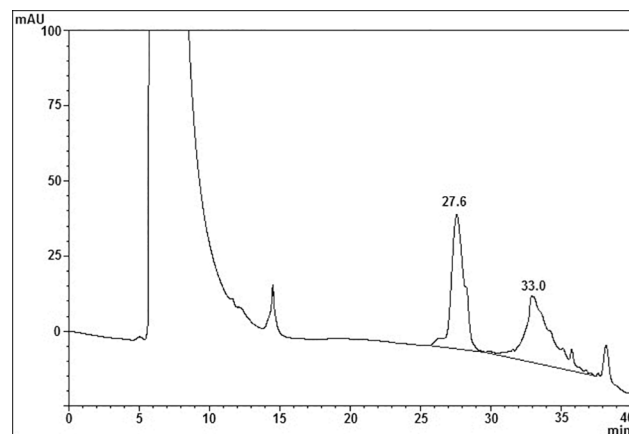
Fig 9. RP-HPLC, run under dissociating conditions as described [64], after application of a sample of ag-FSH obtained from HPSEC (see Fig 8) and incubated overnight with 5M acetic acid at 37°C.

https://doi.org/10.1371/journal.pone.0183545.g009

It is noteworthy, moreover, that ag-GTHα [36], ag-FSHβ and ag-LHβ show 67%, 45% and 51%, respectively, sequence identity with the corresponding human mature peptides and 66%, 67% and 63% with rat mature peptides. These identity values, of the same order as those existing between the human and rat sequences (72%, 65% and 63%), point, in our opinion, to a possible *in vivo* bioactivity detection for ag-FSH and ag-LH if analyzed in the classical female and male rat assay, normally carried out for human gonadotrophic hormone potency determination [77,78]. This is, however, only a hypothesis that needs to be experimentally verified with the purified recombinant hormones.

In our FSHβ alignment considering 41 species (Fig 2), only 14 positions are totally identical, 9 of which being cysteines. Two out of the three remaining conserved cysteines (the 10th and 11th) can be found, however, in 40 of the fish sequences analyzed here, except in *Danio rerio*. The last non-conserved cysteine (the 3rd) is equivalent to the third tetrapod cysteine and, according to several authors, is present in ancient fish such as elasmobranchs [79], chondrosteans [80], eels [69] and Ostariophysi (Siluriformes and Cypriniformes), but not in Salmoniformes and Acanthomorpha (Acanthopterygii and Paracanthopterygii). The present alignment thus confirms these reports, since A. gigas, an ancient fish, also presents the 3rd cysteine as in tetrapods.

Particular cases of FSHβ are *Clarias gariepinus* (Siluriformes), which lost the first N-glycosylation site, and the acanthopterygians species (*Epinephelus coioides*, *Sebastes schlegeli*, *Pseudolabrus sieboldi*, *Trachurus japonicus*), which lack any conserved N-linked sites. Additionally, unlike the other euteleosts, *Gadus morhua* lost the first but not the second putative N-glycosylation site.

Glycosylation is the most abundant post-translational modification of proteins and its impact may range from very subtle to crucial, since glycoproteins are involved in various biological roles. Based on the linkage between the amino acid and the sugar, glycosylation is classified into five types in eukaryotes, the most common being the N- and O-linked glycosylations [81]. Until now, only N-linked glycosylation was described for FSHβ and LHβ and these sites are highly conserved through Osteichthyes evolution, indicating their importance for these proteins; some fish species lack, however, this type of glycosite. N-linked glycosylations present the well-established consensus sequence N-X-S/T (X been any amino acid except Pro) [82,83], while the O-linked glycosylation, which occurs on the OH groups of Serine (S) or Threonine (T), is not known to occur in any consensus sequence in eukaryotes so far, which makes its prediction more difficult.

When comparing the *A. gigas* FSHβ and LHβ peptide sequences with those of other fishes, the lowest identities were found with Acanthomorpha orders (especially Gadiformes) and the highest identities with the basal teleosts Anguilliformes and Ostariophysi (Cypriniformes and Siluriformes). Although at a higher level of conservation, the same pattern was found by Faria et al. [36] comparing the ag-GTHα peptide with other fish orders, varying from 55 to 70% for Acanthomorpha and from 88.1 to 89.5% for Anguilliformes and Ostariophysi. In addition, the comparisons of ag-GTHα with Acipenseriformes (Chondrostei) and Salmoniformes also showed high identity values (87.1% and 75.7%, respectively). This also happens for FSHβ, while LHβ identity between *A. gigas* and the Acipenseriformes is lower than that found for most Acanthomorpha orders. Faria et al. [36] also considered that a relatively well-conserved alpha subunit present in the basal orders of Teleostei and Acipenseriformes gradually evolved to the GTHα forms present in Acanthomorpha.

As for other gonadotrophic hormones, the formation of a "seat-belt" in the β subunit structure that wraps around the α subunit, favored by the disulfide bond existing between an N-terminus (C3) and a C-terminus (C12) cysteine, is also observed in *A. gigas* 3D models [14,45,81]. Chatterjee et al. [84], however, noted that the 3rd conserved cysteine is absent in snakehead fish (*Channa maculata*) FSH and, on the basis of their modeling, suggested that,

thanks to the flexibility of the C-terminal loop, a disulfide bond could be formed between a positionally shifted N-terminal cysteine and the 12th one. In our case it was observed that the electrostatic complementarity of both the α and β subunits in ag-FSH and ag-LH 3D models favors the seat belt formation. Residues included in this seat-belt region (between C10 and C12) have also been shown to be involved in ligand selectivity and in determining receptor specificity. The net charge difference in the region between the 10th and the 11th cysteine residue of the human gonadotropin β-subunit seems, in fact, to have selected FSH receptor-activation from LH receptor-activation [1].

While several studies have performed molecular modeling for human and for other mammalian GTHs, as far as we know only three works reported such models for fish species [66, 84,85]. Particularly interesting is the study carried out by Aizen et al. [66] who analyzed pharmacologically and structurally (3D modeling) the interactions between GTHs and GTHRs of less evolved (eel and trout) and relatively modern (tilapia) fish. The authors highlighted the importance, in receptor activation, of a few residues located outside the hormone-receptor interface region determining diverse electrostatic and steric features in the different species. In the present work, dealing only with ligand and not with receptor models, a difference between the charge distribution in the upper region of the β-subunit of ag-FSH (negatively charged) and that of ag-LH (positively charged) versus a predominantly positive α-subunit is observed. The seat-belt region of both ag-FSHβ and ag-LHβ models displays similar electrostatic features that allow the α-subunit to bind the β-subunit. This equivalent heterodimer formation (and also the similar conformation and electrostatic profile of both α-subunits) is not in contrast with the "negative specificity" model described by Combarnous [86], which states that the common α-subunit could be responsible for receptor high-affinity binding, while the β-subunit for its specificity, determined by inhibiting sites that impede the binding of each dimer to the receptors of the other hormones. It can be suggestive to consider that in our ag-models the top surface of each β-subunit has a different electrostatic distribution. It would be necessary, however, to construct hormone-receptor structural models for ag-GTHs, in order to evaluate whether this change of the electrostatic map in the heterodimer could influence cross-type hormone specificities or cross-species activities.

Particularly interesting in the work of Aizen et al. [66] is the cross-species activation of eel-LHR by tr-LH, which could be explained by the very similar seat-belt sequences of eel-LH and tr-LH (14 identical and 3 similar out of 18 residues), the closest among all GTHs used in the study. As one can observe by adding ag-GTH sequences to the alignment carried out by these authors (S3 Fig), an even higher similarity is found between ag-LH and eel-LH (15 identical and 1 similar residue), or between ag-LH and ta-LH (15 identical and 3 similar), up to the amazing "quasi-identity" found between ag-LH and tr-LH: 17 identical and 1 similar, out of a total of 18 residues. On this basis, therefore, a significant pharmacological activation of eel-LHR, tr-LHR or ta-LHR by ag-LH would be expected. As far as we know, ag-GTHR sequences, which could provide additional hormone-receptor structural models, possibly predicting other cross-species ligand-receptor activations, are not yet available. Finally, still comparing the 3D models of ag-LH and ag-FSH with the human FSH models constructed by Aizen et al. [66], it is worth noting that the calculated fold of *A. gigas* gonadotropin models is very close to the reported human, bovine, porcine and fish fold. These data point to the stability of our proposed models and indicate that the calculated folds corroborate experimental and literature data [48, 50, 66].

It should be noted that the seven proline residues shown in Fig 7, which are totally (C6+13 and C7+11) or partially (C2+1, C5+5, C7+1, C7+6 and C11+7) conserved between the human and *A.gigas* FSH and LH structures, satisfy the predicted secondary structures of the β-subunits of the glycoprotein hormone family reported by Wako and Ishii [85] in their schematic representation. These proline residues are practically all located in β-sheet/loop inversion regions,

confirming the already mentioned tendency of prolines to bend the backbone direction and thus participate in protein folding [72, 87, 88].

The resulting phylogenetic tree of the concatenated FSHβ and LHβ sequences of mature peptide cDNAs placed *A. gigas* (Osteoglossomorpha) as the sister group of Clupeocephala (Ostariophysi and Euteleosteomorpha), while Anguilliformes (Elopomorpha) appears as the earliest diverging branching lineage among teleosts. Siluriformes and Cypriniformes formed a monophyletic group (Ostariophysi), the sister group of Euteleosteomorpha (Acanthomorpha and Salmoniformes). A preliminary synthesis of ag-FSH was carried out in a specific HEK293F^TM cell line suspension culture, in order to ascertain that the cloned transcripts could express the heterodimeric hormone. Identity tests were also performed, leaving no doubt that we were in the presence of the heterodimeric ag-FSH. We must emphasize that no specific immunoassay, antibody or reference standard were available, which made our task quite difficult. Thanks to these results it will now be much easier to synthesize and identify ag-LH and possibly other hormones of this fish species.

In conclusion, this study characterizes the sequences of ag-FSHβ and ag-LHβ peptides, comparing them to those of other teleosts. The 3D models of ag-FSH and ag-LH provided interesting structural comparisons with those reported for other fish GTHs. Additional data for the phylogenetic relationship among Teleostei are provided but they need further confirmation by possibly adding also the ag-TSHβ sequence and using at least three different reconstruction methods (NJ, ML, MP or Bayesian) in order to determine the most reliable tree typology for each β-subunit. The GTHα of *A. gigas* characterized in a previous work and the sequences found here will be used for the biotechnological synthesis of *A. gigas* gonadotrophic hormones. This will be useful for checking the quaternary structures of ag-FSH and ag-LH and their binding to receptors, as well as for physiological and fertility studies and related applications, which are essential for the preservation of this important fish species.

Supporting information

S1 Fig. Root mean squared deviation (RMSD) values of GTHα, FSHβ and LHβ subunits in the respective heterodimers (A); radius of gyration (Rg) of all three subunits in the complexes (B); hydrophobic and hydrophilic surface of two simulated hormones (C) and total number of intra and intermolecular hydrogen bonds of both simulated hormones along the MD simulation (D).
(PDF)

S2 Fig. Root mean squared fluctuation (RMSF) of the α-carbon of the α-subunits (A) and β-subunits (B) of both studied hormones.
(PDF)

S3 Fig. Comparison between the amino acid composition of seat-belts from ag-LH and ag-FSH (present work) and the gonadotropins studied by Aizen et al. [66]. Amino acids were classified as cysteines (pink), negatively charged (red), positively charged (blue), polar (cyan) and hydrophobic (orange)
(PDF)

S4 Fig. Phylogenetic tree of concatenated FSHβ and LHβ DNA sequences obtained by the methods of maximum parsimony (bootstrap values below the branches) and maximum likelihood (bootstrap values above the branches).
(PDF)

S1 Table. Results of primary alignment obtained from HHPRED server.
(PDF)

S2 Table. Average physicochemical parameters obtained from 20ns of molecular dynamics simulation.
(PDF)

S3 Table. Results obtained from Prosa-web, Ramachandran plot and Verify 3D validations for both hormones.
(PDF)

Acknowledgments

Author Contributions

Conceptualization: Thais Sevilhano, Nélio Alessandro de Jesus Oliveira, João Ezequiel Oliveira, Vinicius Gonçalves Maltarollo, Riviane Garcez, Paolo Bartolini.

Data curation: Thais Sevilhano, Roberto Feitosa de Carvalho, Nélio Alessandro de Jesus Oliveira, João Ezequiel Oliveira.

Investigation: Thais Sevilhano, Roberto Feitosa de Carvalho, Nélio Alessandro de Jesus Oliveira, João Ezequiel Oliveira, Vinicius Gonçalves Maltarollo, Gustavo Trossini, Riviane Garcez.

Methodology: Thais Sevilhano, João Ezequiel Oliveira.

Supervision: Thais Sevilhano, João Ezequiel Oliveira, Gustavo Trossini, Paolo Bartolini.

Writing – original draft: Vinicius Gonçalves Maltarollo, Riviane Garcez, Paolo Bartolini.

Writing – review & editing: Paolo Bartolini.

References

1. Levavi-Sivan B, Bogerd J, Mañanós EL, Gómez A, Lareyre JJ. 2010. Perspectives on fish gonadotropins and their receptors. Gen Comp Endocrinol. 2010; 165: 412–437. https://doi.org/10.1016/j.ygcen.2009.07.019 PMID: 19686749

2. Ohta K, Mine T, Yamaguchi A, Matsuyama M. Sexually dimorphic expression of pituitary glycoprotein hormones in a sex-changing fish (Pseudolabrus sieboldi). J Exp Zool Part A. 2008; 309: 534–541.

3. Schulz RW, de França LR, Larteyre JJ, Le Gac F, Chiarini-Garcia H, Nobrega RH, et al. Spermatogenesis in fish. Gen Comp Endocrinol. 2010; 65: 490–411.

4. Senthilkumaran B. Recent advances in meiotic maturation and ovulation: comparing mammals and pisces. Front Biosci. 2011; 16: 1898–1914.

5. Borella MI, Venturieri R, Mancera JM. Immunocytochemical identification of adenohypophyseal cells in the pirarucu (*Arapaima gigas*), an Amazonian basal teleost. Fish Physiol Biochem. 2009; 35: 3–16. https://doi.org/10.1007/s10695-008-9254-x PMID: 18758983

6. Castello L, Stewart DJ, Arantes CC. Modeling population dynamicsand conservation of arapaima in the Amazon Rev Fish Biol Fisher. 2011; 21: 623–640.

7. Chu-Koo F, Dugue R, Aguilar MA, Daza AC, Bocanegra FA, Veintemilla CC, et al. Gender determination in the paiche or pirarucu using plasma vitellogenin, 17 beta-estradiol, and 11-ketotestosterone levels. Fish Physiol Biochem. 2009; 35: 125–136. https://doi.org/10.1007/s10695-008-9211-8 PMID: 19189239

8. Mylonas CC, Fostier A, Zanuy S. Broodstock management and hormonal manipulation of fish reproduction. Gen Comp Endocrinol. 2010; 165: 516–534. https://doi.org/10.1016/j.ygcen.2009.03.007 PMID: 19318108

9. Bousfield GR, Butnev VY, Walton WJ, Nguyen VT, Huneidi J, Singh V, et al. All-hormone N-glycosylation in primate follicle-stimulating hormone β subunits. Mol Cell Endocrinol. 2007; 260: 40–48. https://doi.org/10.1016/j.mce.2006.02.017 PMID: 17079072

10. Carvalho CM, Oliveira JE, Almeida BE, Ueda EKM, Torjesen PA, Bartolini P, et al. Efficient isolation of the subunits of recombinant and pituitary glycoprotein hormones. J Chromatogr A 2009; 1215, 1431–1438.

11. Pierce JC, Parsons F. Glycoprotein hormones: structure and function. Ann Rev Biochem. 1981; 50: 465–495. https://doi.org/10.1146/annurev.bi.50.070181.002341 PMID: 6267989

12. Swanson P, Dickey JT, Campbell B. Biochemistry and physiology of fish gonadotropins. Fish Physiol Biochem. 2003; 28: 53–59.

13. Ulloa-Aguirre A, Zariñan T, Pasapera AM, Casas-Gonzales P, Dias JAQ. Multiple facets of follicle-stimulating receptor function. Endocrine 2007; 32: 251–263. https://doi.org/10.1007/s12020-008-9041-6 PMID: 18246451

14. Boime I, Ben-Menahem D. Glycoprotein hormone structure-function and analog design. Recent Prog Horm Res. 1999; 54: 271–287. PMID: 10548880

15. Butnev VY, Gotschall RR, Butnev VY, Baker VL, Moore WT, Bousfiled GR. Hormone-specific inhibitory influence of α-subunit Asn^{56} oligosaccharide on in vivo subunit association and follicle-stimulating hormone receptor binding of equine gonadotropins. Biol Reprod. 1998; 58: 458–469. PMID: 9475402

16. Suzuki K, Kawauchi H, Nagahama Y. Isolation and characterization of two distinct gonadotropins from chum salmon pituitary glands. Gen Comp Endocrinol. 1988; 71: 292–301. PMID: 3203876

17. Weltzien FA, Kobayashi T, Andersson E, Norberg B, Andersen O. Molecular characterization and expression of FSHβ, LHβ and common α-subunit in male Atlantic halibut (*Hipoglossus hipoglossus*). Gen Comp Endocrinol. 2003; 131: 87–96. PMID: 12679085

18. Kobayashi M, Kato Y, Yishiura Y, Aida K. Molecular cloning of cDNA encoding two types of pituitary gonadotropins alpha subunit from the goldfish *Carassius auratus*. Gen Comp Endocrinol. 1997; 105: 372–378. https://doi.org/10.1006/gcen.1996.6840 PMID: 9073499

19. Yoshiura Y, Kobayashi M, Kato Y, Aida K. Molecular cloning of the cDNAs encoding two gonadotropin β-subunits (GTH-Iβ and -IIβ) from the goldfish, *Carassius auratus*. Gen Comp Endocrinol. 1997; 105: 379–389. https://doi.org/10.1006/gcen.1996.6839 PMID: 9073500

20. Hurvitz A, Degani G, Goldberg D, Din SY, Jackson K, Levavi-Sivan B. Cloning of FSHβ, LHβ, and glycoprotein α-subunits from the russian sturgeon (*Acipenser gueldenstaedtii*), β-subunit mRNA expression, gonad development, and steroid levels in immature fish. Gen Comp Endocrinol. 2005; 140: 61–73. https://doi.org/10.1016/j.ygcen.2004.09.019 PMID: 15596072

21. Kim DJ, Cho YC, Sohn YC. Molecular characterization of rockfish (*Sebastes schlegeli*) gonadotropin subunits and their mRNA expression profiles during oogenesis. Gen Comp Endocrinol. 2005; 141: 282–290. https://doi.org/10.1016/j.ygcen.2005.01.001 PMID: 15804515

22. Choi E, Ko H, Shin J, Kim MA, Sohn YC. Expression of gonadotropin genes in Manchurian trout *Brachymystax lenok* and production of recombinant gonadotropins. Fisheries Sci. 2005; 71: 1193–1200.

23. So W-K, Kwok H-F, Ge W. Zebrafish gonadotropins and their receptors: II. cloning and characterization of zebrafish follicle-stimulating hormone and luteinizing hormone subunits—their spatial-temporal expression patterns and receptor specificity. Biol Reprod. 2005; 72, 1382–1396. https://doi.org/10.1095/biolreprod.104.038216 PMID: 15728794

24. Cerdà J, Chauvigne F, Agulleiro MJ, Marin E., Halm S, Martinez-Rodriguez G, et al. Molecular cloning of Senegalese sole (*Solea senegalensis*) follicle-stimulating hormone and luteinizing hormone subunits and expression pattern during spermatogenesis. Gen Comp Endocrinol. 2008; 156: 470–481. https://doi.org/10.1016/j.ygcen.2008.02.006 PMID: 18353326

25. Huang H, Zhang Y, Huang W, Li S, Zhu P, Liu Y, et al. Molecular characterization of marbled eel (*Anguilla marmorata*) gonadotropin subunits and their mRNA expression profiles during artificially induced gonadal development. Gen Comp Endocrinol. 2009; 162: 192–202. https://doi.org/10.1016/j.ygcen.2009.02.012 PMID: 19327361

26. Cao H, Zhou L, Zhang YZ, Wei QW, Chen XH, Gui JF. Molecular characterization of Chinese sturgeon gonadotropins and cellular distribution in pituitaries of mature and immature individuals. Mol Cell Endocrinol. 2009; 303: 34–42. https://doi.org/10.1016/j.mce.2009.01.015 PMID: 19428989

27. Mittelholzer C, Andersson E, Tarange GL, Karlsen O, Norberg B. Quantification of gonadotropin subunits GPα, FSHβ and LHβ mRNA expression from atlantic cod (*Gadus morhua*) throughout a

reproductive cycle. Comp Biochem Physiol B 2009; 153: 288–295. https://doi.org/10.1016/j.cbpb.2009.03.011 PMID: 19344778

28. Guzman JM, Luckenbach JA, Swanson P. Molecular characterization and quantification of sablefish (*Anoploma fimbria*) gonadotropins and their receptors: reproductive dysfunction in female captive broodstock. Gen Comp Endocrinol. 2013; 193: 37–47. https://doi.org/10.1016/j.ygcen.2013.07.007 PMID: 23892013

29. Kobayashi M, Morita T, Ikeguchi K, Yoshizaki G, Suzuki T, Watabe S. Production of recombinant goldfish gonadotropins by baculovirus in silkworm larvae. Fish Physiol Biochem. 2003; 28: 469–471.

30. Kamei H, Ohira T, Yoshiura Y, Uchida N, Nagasawa H, Aida K. Expression of a biologically active recombinant follicle-stimulating hormone of Japanese eel, *Anguilla japonica*, using methylotropic yeast, *Pichia pastoris*. Gen Comp Endocrinol. 2003; 134: 244–254. PMID: 14636631

31. Kasuto H, Levavi-Sivan B. Production of biologically active tethered tilapia LHβα by the methylotropic yeast *Pichia pastoris* Gen Comp Endocrinol. 2005; 140: 222–232. https://doi.org/10.1016/j.ygcen.2004.10.016 PMID: 15639150

32. Aizen J, Kasuto H, Golan M, Zakay H, Levavi-SivanB. Tilapia follicle-stimulating hormone (FSH): immunochemistry, stimulation by gonadotropin-releasing hormone, and effect of biologically active recombinant FSH on steroid secretion. Biol Reprod. 2007; 76: 692–700. https://doi.org/10.1095/biolreprod.106.055822 PMID: 17192515

33. Yu X, Lin S, Kobayashi M, Ge W. Expression of recombinant zebrafish follicle-stimulating hormone (FSH) in methylotropic yeast *Pichia pastoris*. Fish Physiol Biochem. 2010; 36: 273–281. https://doi.org/10.1007/s10695-008-9244-z PMID: 20467863

34. Kazeto Y, Kohara M, Miura T, Yamaguchi S. Trant JM, Adachi S, et al. Japanese eel follicle-stimulating hormone (Fsh) and luteinizing hormone (Lh): production of biologically active recombinant Fsh and Lh by *Drosophila* S2 cells and their differential actions on the reproductive biology. Biol Reprod. 2008; 79: 938–946. https://doi.org/10.1095/biolreprod.108.070052 PMID: 18685126

35. Zmora N, Kazeto Y, Kumar RS, Schülz RW, Trant JM. Production of recombinant channel catfish (*Ictalurus punctatus*) FSH and LH in S2 *Drosophila* cell line and an indication of their different actions. J Endocrinol. 2007; 194: 407–416. https://doi.org/10.1677/JOE-07-0171 PMID: 17641288

36. Faria MT, Carvalho RF, Sevilhano TCA, Oliveira NAJ, Silva CFP, Oliveira JE, et al. Isolation of the pituitary gonadotrophic α-subunit hormone of the giant Amazonian fish: pirarucu *(Arapaima gigas)*. Fish Phys Biochem. 2013; 39, 683–693.

37. Hall TA. BioEdit: a user-friendly biological sequence alignment editor and analysis program for Windows 95/98/NT. Nucl Acids Symp Ser. 1999; 41: 95–98.

38. Petersen TN, Brunak S, Heijne GV, Nielsen H. SignalP 4.0: discriminating signal peptides from transmembrane regions. Nat. Methods 2011; 8: 785–786 https://doi.org/10.1038/nmeth.1701 PMID: 21959131

39. Chotia C, Lesk M. The relation between the divergence of sequence and structure in proteins. EMBO J. 1986; 5: 823–826. PMID: 3709526

40. Holm L, Sander C. Protein structure comparison by alignment of distance matrices. J Mol Biol. 1993; 233: 123–138. https://doi.org/10.1006/jmbi.1993.1489 PMID: 8377180

41. Soding J, Biegert A, Lupas AN. The HHpred interactive server for protein homology detection and structure prediction. Nucleic Acids Res. 2005; 33: 244–248. https://doi.org/10.1093/nar/gki162

42. Sali A, Blundell TL. Comparative protein modelling by satisfaction of spatial restraints. J. Mol. Biol. 1993; 234: 779–815. https://doi.org/10.1006/jmbi.1993.1626 PMID: 8254673

43. Eswar N, Marti-Renom MA, Webb B, Madhusudhan MS, Eramian D, Shen M, et al. Comparative Protein Structure Modeling with MODELLER. Current Protocols in Bioinformatics, John Wiley & Sons, Inc., Supplement 15; 2006. pp. 5.6.1–5.6.30.

44. Marti-Renom MA, Stuart A, Fiser A, Sánchez R, Melo F, Sali A. Comparative protein structure modeling of genes and genomes. Annu Rev Biophys Biomol Struct. 2000; 29: 291–325. https://doi.org/10.1146/annurev.biophys.29.1.291 PMID: 10940251

45. Lapthorn AJ, Harris DC, Littlejohn A, Lustbader JW, Canfield R., Machin KJ, et al. Crystal structure of human chorionic gonadotropin. Nature 1994; 369-455–461. https://doi.org/10.1038/369455a0 PMID: 8202136

46. Jiang X, Liu H, Chen X, Chen P-H, Fischer D, Sriraman V, et al. Structure of follicle-stimulating hormone in complex with the entire ectodomain of its receptor. PNAS 2012; 109: 12491–12496. https://doi.org/10.1073/pnas.1206643109 PMID: 22802634

47. Wu H, Lustbader JW, Liu Y, Canfield RE, Hendrickson W. Structure of human chorionic gonadotropin at 2.6 A resolution from MAD analysis of the selenomethionyl protein. Structure 1994; 2: 545–58. PMID: 7922031

48. Lovell SC, Davis IW, Adrendall WB, de Bakker PIW, Word JM, Prisant MG, et al. Structure validation by Calpha geometry: phi, psi and Cbeta deviation. Proteins 2002; 50: 437–450.

49. Berendsen HJC, Van der Spoel D, Van Drunen R. GROMACS: A message-passing parallel molecular dynamics implementation. Comp Phys Commun. 1995; 91: 43–56.

50. Lindahl E, Hess B, Van der Spoel B. GROMACS 3.0: a package for molecular simulation and trajectory analysis. J Mol Mod. 2001; 7: 306–317.

51. Van Gunsteren W F, Billeter SR. Biomolecular Simulations: The GROMOS96 Manual and User Guide. Zürich, VdF Hochschulverlag ETHZ; 1996.

52. Fan H, Mark AE. Refinement of homology-based protein structures by molecular dynamics simulation techniques. Protein Sci. 2004; 13: 211–220. https://doi.org/10.1110/ps.03381404 PMID: 14691236

53. Lüthy R, Bowie JU, Eisenberg D. Assessment of protein models with three-dimensional profiles. Nature 1992; 35: 83–5.

54. Wiederstein M, Sippl MJ. ProSA-web: interactive web service for the recognition of errors in three-dimensional structures of proteins. Nuc. Acids Res. 2007; 35: W407–W410.

55. Sant'Ana C D, Bernarde CP, Izidoro LFM, Mazzi MV, Soares SG, Fuly AL, et al. Molecular characterization of BjussuSP-I, a new thrombin-like enzyme with procoagulant and kallikrein-like activity isolated from Bothrops jararacussu snake venom. Biochimie 2008; 90-500–507. https://doi.org/10.1016/j.biochi.2007.10.005 PMID: 17996740

56. Zaqueo KD, Kayano AM, Simões-Silva R, Moreira-Dill LS, Fernandes CFC, Fuly AL, Maltarollo VG, et al. Isolation and Biochemical Characterization of a New Thrombin-Like Serine Protease from Bothrops pirajai Snake Venom. BioMed Res Intern, Article ID 595186, 13 pages, 2014. https://doi.org/10.1155/2014/595186 PMID: 24719874

57. Martins W, Baldasso PA, Honório KM, Maltarollo VG, Ribeiro RIMA, Carvalho BMA. A Novel Phospholipase A2 (D49) from the Venom of the Crotalus oreganus abyssus (North American Grand Canyon Rattlesnake). BioMed Research International, Article ID 654170, 15 pages, 2014. https://doi.org/10.1155/2014/654170 PMID: 24707493

58. Edgar RC. MUSCLE: multiple sequence alignment with high accuracy and high throughput. Nucl Acids Res. 2004; 32: 1792–1797. https://doi.org/10.1093/nar/gkh340 PMID: 15034147

59. Tamura K, Stecher G, Peterson D, Filipski A, Kumar S. MEGA6: molecular evolutionary genetics analysis version 6.0. Mol Biol Evol. 2013; 30: 2725–2729. https://doi.org/10.1093/molbev/mst197 PMID: 24132122

60. Hasegawa M, Kishino H, Yano T. Dating the human-ape split by a molecular clock of mitochondrial DNA. J Mol Evol.1985; 22: 160–174. PMID: 3934395

61. Felsenstein J. Confidence limits on phylogenies: an approach using the bootstrap. Evolution 1985; 39: 783–791. https://doi.org/10.1111/j.1558-5646.1985.tb00420.x PMID: 28561359

62. Loureiro RF, Oliveira JE, Torjesen PA, Bartolini P, Ribela MTCP. Analysis of intact human follicle-stimulating hormone preparations by reversed-phase high-performance liquid chromatography. J Chromatogr A 2006; 1136: 10–18. https://doi.org/10.1016/j.chroma.2006.09.037 PMID: 17049544

63. Almeida BE, Damiani R, Oliveira JE, Dalmora SL, Torjesen PA, Bartolini P, Ribela MTCP. Reversed-phase high performance liquid chromatography as na alternative to animal bioassay for human thyrotropin potency determination. Anal Methods 2014; 6: 6688–6694.

64. Carvalho CM, Oliveira JE, Almeida BE, Ueda EKM, Torjesen PA, Bartolini P, Ribela MTCP. Efficient isolation of the subunits of recombinant and pituitary glycoprotein hormones. J Chromatogr A 2009; 1216: 1431–1438. https://doi.org/10.1016/j.chroma.2008.12.096 PMID: 19167716

65. Sheets MD, Ogg SC, Wickens MP. Point mutations in AAUAAA and in the poly (A) addition site: effects on the accuracy and efficiency of cleavage and polyadenylation in vitro. Nucl Acids Res. 1990; 18: 5799–5805. PMID: 2170946

66. Aizen J, Kowalsman N, Kobauashi M, Hollander L, Chang Sohn Y, Yoshizaki G, Niv MY, Levavi-Sivan B. Experimental and computational study of inter- and intra- species specificity of gonadotropins for various gonadotropin receptors. Mol Cell Endocrinol. 2012; 364: 89–100. https://doi.org/10.1016/j.mce.2012.08.013 PMID: 22954681

67. Kawauchi H, Sower SA. The dawn and evolution of hormones in the adenohypophysis. Gen Comp Endocrinol. 2006; 148: 3–14. https://doi.org/10.1016/j.ygcen.2005.10.011 PMID: 16356498

68. Li MD, Ford JJ. A comprehensive evolutionary analysis based on nucleotide and amino acid sequences of the α- and β-subunits of glycoprotein hormone gene family. J Endocrinol. 1998; 156: 529:542. PMID: 9582510

69. Degani G, Goldberg D, Tzchori I, Hurvitz A, Din SY, Jackson K. Cloning of European eel (*Anguilla anguilla*) FSH-β subunit, and expression of FSH-β and LH-β in males and females after sex determination. Comp Biochem Physiol. B 2003; 136: 283–293. PMID: 14529754

70. Fan QR, Hendrickson WA. Structure of human follicle-stimulating hormone in complex with its receptor. Nature 2005; 433: 269–277. https://doi.org/10.1038/nature03206 PMID: 15662415

71. Baldwin RL. 2008. The search for folding intermediates and the mechanism of protein folding. Annu Rev Biophys. 2008; 37: 1–21. https://doi.org/10.1146/annurev.biophys.37.032807.125948 PMID: 18573070

72. Morgan AA, Rubenstein E. Proline: the distribution, frequency, positioning, and common functional roles of proline and polyproline sequences in the human proteome. PLoS ONE 2013; 8: e53785. https://doi.org/10.1371/journal.pone.0053785 PMID: 23372670

73. Xing Y, Myers RV, Cao D, Lin W, Jiang M, Bernard MP, et al. 2004. Glycoprotein hormone assembly in the endoplasmic reticulum: III. the seatbelt and its latch site determine the assembly pathway. J Biol Chem. 2004; 279: 35449–35457. https://doi.org/10.1074/jbc.M403054200 PMID: 15161904

74. Campbell R, Dean-Emig D, Moyle W. 1991. Conversion of human choriogonadotropin into a follitropin by protein engineering. P Natl Acad Sci. USA 1991; 88: 760–764.

75. Dias JA, Zhang YQ, Liu XX. Receptor-binding and functional-properties of chimeric human follitropin prepared by an exchange between a small hydrophilic intercysteine loop of human follitropin and human lutropin. J Biol Chem. 1994; 269: 25289–25294. PMID: 7929221

76. Grossmann M, Szkudlinski MW, Wong R, Dias JA, Ji TH, Weintraub BD. Substitution of the seat-belt region of the thyrotropin (TSH) β-subunit with the corresponding regions of choriogonadotropin or follitropin confers luteotropic but not follitropic activity to chimeric TSH. J Biol Chem. 1997; 272: 15532–15540. PMID: 9182589

77. Steelman SL, Pohley FM. Assay of the follicle-stimulating hormone based on the augmentation with human chorionic gonadotropin. Endocrinology 1953; 53: 604–614. https://doi.org/10.1210/endo-53-6-604 PMID: 13116950

78. Storring PL, Gaines Das RE. The fourth international standard for human urinary FSH and LH: specificities of LH seminal vesicle weight gain assays in the collaborative study differ between laboratories. J Endocrinol. 2001; 171: 119–129. PMID: 11572796

79. Querat B, Tonnerre-Doncarli C, Genies F, Salmon C. Duality of gonadotropins in gnathostomes. Gen Comp Endocrinol. 2001; 124: 308–314. https://doi.org/10.1006/gcen.2001.7715 PMID: 11742514

80. Querat B, Sellouk A, Salmon C. Phylogenetic analysis of the vertebrate glycoprotein hormone family including new sequences of sturgeon (*Acipenser baeri*) β-subunits of the two gonadotropins and the thyroid-stimulating hormone. Biol Reprod. 2000; 63: 222–228. PMID: 10859263

81. Chauhan JS, Rao A, Raghava GPS. In silico platform for prediction of N-, O- and C-glycosites in eukaryotic protein sequences. Plops One 2013; 8: e67008.

82. Gavel Y, von Heijne G. Sequence differences between glycosylated and non-glycosylated Asn-X-Thr/Ser acceptor sites: implications for protein engineering. Protein Eng. 1990; 3: 433–442. PMID: 2349213

83. Lehle L, Tanner W. 1978. Glycosyl transfer from dolichyl phosphate sugars to endogenous and exogenous glycoprotein acceptors in yeast. Eur J Biochem. 1978; 83: 563–570. PMID: 344041

84. Chatterjee A, Shen S-T, Yu JY-L. Molecular cloning of cDNAs and structural model analysis of two gonadotropin β-subunits of snakehead fish (Channa maculata). Gen Comp Endocrinol. 2005; 143: 278–286. https://doi.org/10.1016/j.ygcen.2005.04.004 PMID: 15922345

85. Aizen J, Kowalsman N, Niv MY, Levavi-Sivan B. Characterization of tilapia (*Oreochromis niloticus*) gonadotropins by modeling and immunoneutralization. Gen Comp Endocrinol. 2014; 207: 28–33. https://doi.org/10.1016/j.ygcen.2014.05.028 PMID: 24954479

86. Combarnous Y. Molecular basis of the specificity of binding of glycoprotein hormones to their receptors. Endocr Rev. 1992; 13: 670–691. https://doi.org/10.1210/edrv-13-4-670 PMID: 1281088

87. Wako H, Ishii S. 1995. Secondary structure prediction of β-subunits of the gonadotropin-thyrotropin family from its aligned sequences using environment-dependent amino-acid substitution tables and conformational propensities. Biochim Biophys Acta 1995; 1247: 104–112. PMID: 7873578

88. Han Y-S, Yu Y-L. Molecular cloning and sequence analysis of the cDNAs for pituitary glycoprotein hormone α subunits from two species of synbranchiformes, *Monopterus albus* and *Ophisternon bengalense*. Fish Physiol Biochem. 2002; 26: 111–120.